Joint Altitude and Hybrid Beamspace Precoding Optimization for UAV-Enabled Multiuser mmWave MIMO System

Zhen Chen, *Member, IEEE*, Nan Zhao, *Senior Member, IEEE*, Daniel Ka Chun So, *Senior Member, IEEE*, Jie Tang, *Senior Member, IEEE*, Xiu Yin Zhang, *Fellow, IEEE*, and Kai-Kit Wong, *Fellow, IEEE*

***Abstract*—The combination of unmanned aerial vehicles (UAVs) and millimeter wave (mmWave) multiple-input multiple-out (MIMO) system is regarded as a key enabling technology for beyond 5G networks, as it provides high data rate aerial links. However, establishing UAV-enabled mmWave MIMO communication is quite challenging due to the high hardware cost in terms of radio frequency (RF) chains. As a cost-effective alternative, a beamspace precoding with discrete lens arrays (DLA) architecture has received considerable attention. However, the underlying optimal design in beamspace precoding has not been fully exploited in UAV-enabled communication scenario. In this paper, the joint design of the UAV's altitude and hybrid beamspace precoding is proposed for the UAV-enabled multiuser MIMO system, in which the DLA is exploited to reduce the number of the RF chain. In the proposed scheme, the optimization problem is formulated as a minimum weighted mean squared error (MWMSE) method. Then an efficient algorithm with the penalty dual decomposition (PDD) is proposed that aims to jointly optimize the altitude of UAV, beam selection and digital precoding matrices. Simulation results confirm the comparable performance of the proposed scheme and perform close to full-digital beamforming in terms of achievable spectral efficiency.**

Manuscript received July 10, 2021; revised October 12, 2021 and November 29, 2021; accepted November 30, 2021. Date of publication December 13, 2021; date of current version February 14, 2022. This work was supported in part by National Key Research and Development Project under Grant 2019YFB1804100, in part by the National Natural Science Foundation of China under Grants 61971194 and 62001171, in part by the Key Research and Development Project of Guangdong Province under Grant 2019B010156003, in part by the Natural Science Foundation of Guangdong Province under Grants 2019A1515011607 and 2021A1515011966, in part by the Open Research Fund of National Mobile Communications Research Laboratory, Southeast University under Grant 2019D06, in part by Guangxi Technology Basement and Talent Program under Grant 2020AC15010. The review of this article was coordinated by Prof. Jingon Joung. *(Corresponding author: Jie Tang.)*

Zhen Chen and Xiu Yin Zhang are with the School of Electronic and Information Engineering, South China University of Technology, Guangzhou 510641, China (e-mail: chenz@scut.edu.cn; zhangxiuyin@scut.edu.cn).

Nan Zhao is with the School of Information and Communication Engineering, Dalian University of Technology, Dalian 116024, China (e-mail: zhaonan@dlut.edu.cn).

Daniel Ka Chun So is with the School of Electrical and Electronic Engineering, University of Manchester, M139PL Manchester, U.K. (e-mail: d.so@manchester.ac.uk).

Jie Tang is with the School of Electronic and Information Engineering, South China University of Technology, Guangzhou 510641, China, and also with the National Mobile Communications Research Laboratory, Southeast University, Nanjing 210096, China (e-mail: eejtang@scut.edu.cn).

Kai-Kit Wong is with the Department of Electronic and Electrical Engineering, University College London, WC1E6BT London, U.K. (e-mail: kai-kit.wong@ucl.ac.uk).

Digital Object Identifier 10.1109/TVT.2021.3134044

***Index Terms*—UAV, mmWave communication, MIMO, hybrid beamspace precoding, lens antenna arrays.**

I. Introduction

UNMANNED aerial vehicles (UAVs) have recently proven to be of immense help in both military and civilian fields and can be endowed with multiple-input-multiple-output (MIMO) for wireless communication networks. Different from terrestrial communications, UAVs can provide an ondemand flexible platform for deploying aerial base station (BS) to support temporary or urgent events, which enhances the wireless capacity for ground terminals (GTs) [1], [2]. Particularly, UAVs are used to provide various services, such as sampling data from dangerous areas, firefighting and disaster rescue [3]. In addition, UAVs are envisioned to be a prime candidates of future mmWave communication systems [4]. Because of the short wavelength at mmWave frequency, massive antenna arrays can be deployed on a UAV to form the beam-steerable directive beam, which is witnessed as a promising approach to offer available data rates and extensive coverage [5], [6]. However, the desired beamforming gains in conventional UAV-enabled system tend to rely on the fully digital precoding structure, where one radio frequency (RF) chain is required to serve one antenna [7]. An increase in RF chain has resulted in high hardware cost, which obstruct the commercial deployment of UAV-enabled mmWave MIMO systems [8]. It has been proven that RF chains may consume up to 70% of the total transceiver power [7], [9]–[11]. Therefore, high hardware cost (RF chain) makes the UAV-enabled mmWave MIMO system unrealistic to low-cost communications.

To tackle this challenge, lots of studies have been developed to reduce the energy consumption and the number of RF chains, such as load-controlled parasitic antenna arrays (LC-PAAs) [12], [13], beam selection [14]–[17] and hybrid analog/digital precoding design [18]–[22]. The recent concept of "*beamspace MIMO*" has been exploited as a potential scheme to substantiality reduce the hardware cost of RF chains, where the discrete lens array (DLA) is considered for analog spatial beamforming [23], [24]. In a beamspace MIMO systems, the electromagnetic (EM) lens with the antenna array are developed for analog spatial beamforming domain [23]. To compensate the high attenuation of mmWave frequencies, the different directions of mmWave signals can be focused on the antenna array, which is referred

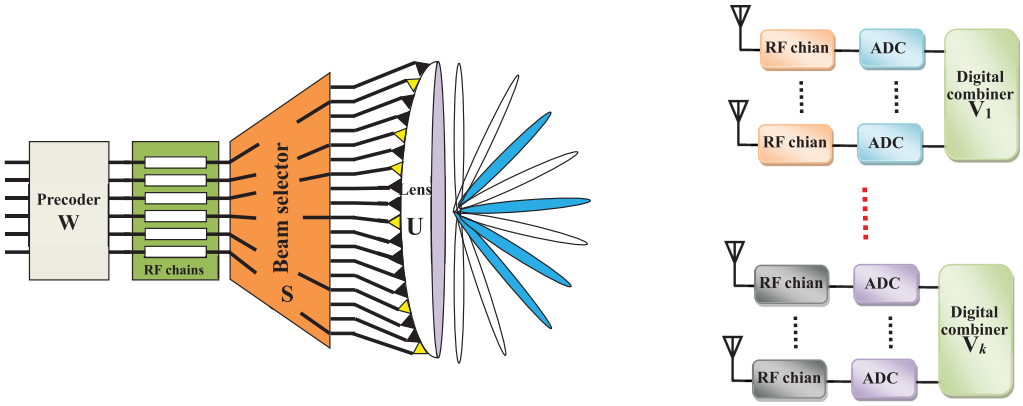

Fig. 1. Illustration of the mmWave MIMO communication with the LAAs.

to as *beamspace channel* [25]. Due to the high path loss at mmWave frequencies, the beamspace mmWave channel with lens antenna array (LAA) is sparse, meaning that only a part of beams carry the majority of the information [26]. Thus the beam selector is designed to determine the energy-focusing beams, which can reduce the required number of RF chains with only a negligible performance degradation [27], [28]. However, the beam selection is not a trivial task. The traditional beam selection problem is maximum magnitude (the works in "MM-BS") so as to obtain a higher transmission rate. Subsequently, [29] designs an interference-aware precoding strategy for multiuser interference system, which is simpler and less expensive than the MM-BS schemes. However, these works are restricted to the terrestrial communications, where the beam selection techniques are developed for mmWave MIMO systems primarily considered a static or quasi-static scenario. It is commonly believed that the mmWave MIMO systems with fixed infrastructure are vulnerable to unforeseen or temporary events (e.g., natural disasters, sports events). Therefore, it is important to develop the UAV-enabled beamspace precoding schemes to deal with emergencies promptly.

A. Related Works and Motivation

There are a recent surge of studies on the use of UAVs for mmWave communications [5], [30]–[34]. To assess the applicability of UAV deployment in mmWave system, it is critical to design a comprehensive and efficient hybrid beamforming (HBF), while also taking into account the effects of mmWave high attenuation propagation. However, one major drawback of the hybrid analog/digital precoding is the requirement of a large number of RF chains and phase shifters, which lead to extra power consumption and hardware cost [22]. It should be noted that the hybrid precoding/combining matrices optimization problem is more difficult and complicated than the traditional fully digital one [33]–[35]. One effective and commonly used approach is to exploit the energy-focusing capability of lens, such hybrid analog/digital transceiver architecture is designed as shown in Fig. 1. The key idea is to exploit the DLA for mmWave MIMO communications. In [24], a path division multiplexing (PDM) paradigm was introduced in DLA-based mmWave MIMO system, where parallel data streams were transmitted over different propagation paths. In [36], the full-dimensional DLA-based mmWave system was developed in multi-user mmWave scenarios using a path division multiple access strategy. In [37], the high-dimensional DLA for the beamspace MIMO system was investigated and was then extended to the high-dimensional multiuser communication scenarios [38]. In beamspace MIMO system, beam selection scheme often was studied to significantly reduce the RF complexity while obtaining near-optimal performances [7]. However, the same beam at the BS is likely selected for different users, which may cause inter-user interference in the beamspace MIMO system. To tackle this problem, an interference-aware scheme for beam selection was investigated in [29]. Subsequently, the compressed channel estimation was studied in mmWave beamspace MIMO system by exploiting the structure of LAAs [39]. It is worth noting that the beamspace MIMO system is essentially similar to the phase shifting and selection in dynamic hybrid precoding system [40], but the beamspace MIMO uses analog to digital converters (ADCs) to significantly lower hardware cost and alleviate the performance bottleneck caused by the multi-user interference. Therefore, applying DLA to UAV-enabled wireless communication will have tremendous potential.

However, the hybrid beamspace precoding optimization scheme for UAV-enabled mmWave MIMO communication is still an open problem. The primary concern for UAV-enabled mmWave MIMO system is that the altitude of UAV and the beam selector with LAAs will make the problem highly non-convex and difficult to solve. In addition, the joint optimizing transmit precoder and receive combiners often are coupled with each other. Most of the existing works focus on simple decoupling mechanisms, in which the original optimization problem is divided into transmit and receive precoding subproblems, and then focus on the constant modulus constraint in solving the subproblems. These techniques are effective but follow a heuristic design way. Moreover, such decoupling mechanisms may result in a performance loss in some cases, since a fixed digital precoder is usually not optimal. In addition, these prior works are restricted to terrestrial communications whose results do not consider the presence of UAVs. This motivates our work

to propose more efficient techniques for UAV-enabled mmWave communications.

B. Main Contributions

The integration of UAV and *beamspace MIMO* is viewed as a promising technique in the upcoming mmWave communication, and hence has drawn great interests recently. Most of the prior art on UAV-enabled mmWave MIMO system [30]–[34] does not consider the LAAs to substantially reduce the RF chains and the power consumption. In particular, these known approaches are restricted to phase shifters whose results cannot be extended directly to UAV-enabled mmWave beamspace MIMO systems. In addition, the works in [29], [36]–[38], [40] proposed the joint optimizing transmit and receive beamforming scheme for mmWave beamspace MIMO system that minimize mean squared error (MSE) or maximize the sum-rate. However, these works do not consider the presence of UAV. Especially, in practical UAV-enabled communication scenarios, the random movement of the UAV will result in the appearance and disappearance of scatterers, which lead to a considerable performance loss. Therefore, jointly optimizing the altitude of UAV and hybrid beamspace precoding in UAV-enabled mmWave MIMO communication is a problem worth investigating and exploring. Motivated by the above studies, this work proposes the joint optimization of altitude of UAV, the beam selection and beamspace precoding for UAV-enabled mmWave MIMO system. The contributions in this article can be summarized as follows.

- Firstly, an efficient joint optimization approach is proposed for UAV-enabled mmWave beamspace MIMO system. Apart from the above mentioned challenges in the existing joint optimization problem, the altitude of UAV, the digital precoder/combiner variables and the location planning are also considered in the UAV-enabled mmWave scenario.
- The proposed optimization problem is NP-hard, which makes it difficult to achieve acceptable results. To tackle this problem, the penalty dual decomposition (PDD) method is considered by introducing a series of equality constraints with auxiliary variables and penalty hyperparameters to cope with the coupling digital precoding/combining matrices and beam selector constraints. After that the optimization problem is reformulated as equivalent augmented Lagrangian (AL) function, and seeks its minimizer via an AL method, where each subproblem is solved independently by using the block coordinate descent (BCD) algorithm.
- To achieve the optimal flight altitude of UAV, a low-complexity scheme is proposed, where the two cases are distinguished by checking whether the given altitude is sufficient for the UAV to serve its associated GTs. Numerical results validate the effectiveness of the proposed strategy of jointly optimizing the altitude of UAV, beam selection and hybrid precoding/combining matrices, and achieve a satisfactory performance close to that of the full digital precoder.

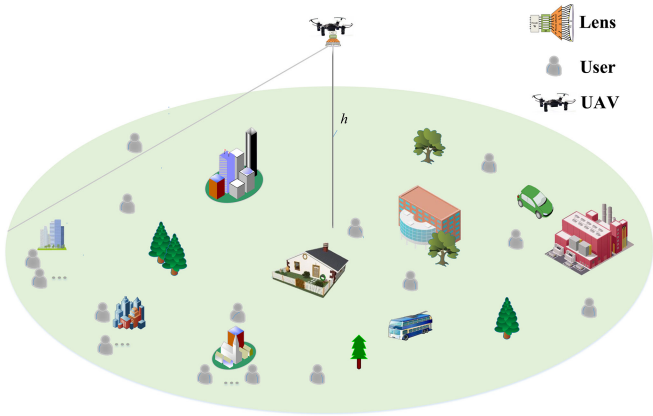

Fig. 2. Illustration of a UAV-enabled hybrid beamspace beamforming for multiuser mmWave communication systems.

C. Organization and Notation

The remain of this paper is organized as follows. The Section II presents the system model of a multi-user mmWave beamspace system along with the joint optimization problem formulation. In Section III, we present the basic idea and the optimization procedure. In Section IV, the simulation results are provided to validate the theoretical findings, followed by the conclusions in Section V.

Notations: Scalar is denoted by lower-case letters; lower- and upper-case boldface letters are used for vectors and matrices, respectively; $\mathrm{tr}(\cdot)$ is the trace of a matrix; $\log(\cdot)$ is used for the logarithm; $\boldsymbol{I}_K$ denotes the $K \times K$ identity matrix; The superscripts $(\cdot)^T$, $(\cdot)^H$, denote the transpose and conjugate transpose, respectively; $\mathfrak{Re}\{\mathbf{x}\}$ and $\mathbf{x}^H$ are the real part and conjugate of a complex signal $\mathbf{x}$, respectively; $(\cdot)_j$ is denoted by the j-th column of a matrix; $(\cdot)_{i,j}$ denotes i,j-th element of a matrix; $\mathcal{CN}(m,\sigma^2)$ represents the symmetric complex-valued Gaussian distributions with mean m and covariance σ^2; $\|\cdot\|_2$, $\|\cdot\|_F$, $\mathrm{diag}(\cdot)$ and $\mathbb{E}[\cdot]$ denote the Euclidean norm, Frobenius norm, diagonalization and expectation operators, respectively.

II. Problem Formulation

We describe a downlink mmWave beamspace communication, where a UAV is deployed as a flying base-station (BS) to serve K simultaneous GTs in Fig. 2. The UAV is equipped with LAAs. We assume that the UAV with horizontal and vertical position $\mathbf{x} = (x(1), x(2))$ is hovering at altitude of h meters above the ground level. The height of each GT is assumed to be zero compared with the height of the UAV. $\mathbf{z}_k = (z_k(1), z_k(2))$ is used for the location of GT k. Thus, the ground coverage area of the UAV depend on the antenna's main lobe with radius $\|\mathbf{z} - \mathbf{x}_k\|_2 = h\mathbf{tan}\Theta$. The UAV with N_t transmit antennas and N_t^{RF} RF chains serves a total of K GTs each of which is equipped with N_r receive antennas. It is assumed that N_s data streams are transmitted to a receiver, which are subject to constraints $KN_s \leq N_t^{RF} < N_t$ and $N_s \leq N_r$.

Due to the sparsity and high free-space path loss at mmWave band, we consider the Rician fading channel model [41]. Different from the conventional low frequency channels, the mmWave

channels between UAV and GTs are stochastic fading, and thus the channel matrix from the *k*-th GT to the UAV can be expressed as [42]

$$\hat{\boldsymbol{H}}_k = \sqrt{\beta_0 (d_k)^{-\alpha}} \left(\sqrt{\frac{\delta}{\delta+1}} G_k + \sqrt{\frac{1}{\delta+1}} \hat{G}_k \right), \quad (1)$$

where β_0 is the channel power gain, $d_k = \sqrt{\|\mathbf{z} - \mathbf{x}_k\|_2^2 + h^2}$ is the distance between the UAV and GT k and $\alpha \geq 2$ denotes the path loss exponent. G_k is the LoS component of the GT k with $G_k(i,j) = 1$, $\hat{G}_k$ denotes the the Rayleigh fading channel (or NLoS) component of the GT k and $\delta \geq 0$ is the Rician factor specifying the power ratio between the dominant LoS and NLoS components.

A. The Lens-Aided Mmwave MIMO System

As shown in Fig. 1, the lens antenna arrays are designed on the UAV-enabled mmWave MIMO system. In this structure, the signals arriving from different unknown directions will be focused on the array antennas. Such the lens $\boldsymbol{U}$ can be characterized as a spatial discrete fourier transform of the incident signals, which includes the array steering vectors of N_t covering the entire angular domain as follows [43]

$$\boldsymbol{U} = \left[\mathbf{a}(\overline{\phi}_1), \mathbf{a}(\overline{\phi}_2), \ldots, \mathbf{a}(\overline{\phi}_{N_t}) \right]^H, \quad (2)$$

where $\mathbf{a}(\overline{\phi}_i) = \frac{1}{\sqrt{N_t}} [e^{-2j\pi\overline{\phi}_i n}]_{n \in \mathcal{I}}$ is the $N_t \times 1$ array steering vector for the spatial direction $\overline{\phi}_i$, and $\mathcal{I} = \{n - (N_t - 1)/2 | n = 0, 1, \ldots, N_t - 1\}$ is an index set of array elements. $\overline{\phi}_i$ is the normalized spatial directions [21]

$$\overline{\phi}_i = \frac{1}{N_t} \left(i - \frac{N_t - 1}{2} \right), \quad i = 1, 2, \ldots, N_t. \quad (3)$$

Thus, the physical spatial MIMO channel $\hat{\boldsymbol{H}}_k$ in (1) can be obtained with the Fourier transformation, which is defined as [24]

$$\tilde{\boldsymbol{H}}_k = \hat{\boldsymbol{H}}_k \boldsymbol{U} = (d_k)^{-\frac{\alpha}{2}} \boldsymbol{H}_k. \quad (4)$$

where $\boldsymbol{H}_k = \sqrt{\frac{\beta_0 \delta}{\delta+1}} \boldsymbol{G}_k \boldsymbol{U} + \sqrt{\frac{\beta_0}{\delta+1}} \hat{\boldsymbol{G}}_k \boldsymbol{U}$.

For each GT, the received signal is processed with a digital combiner $\boldsymbol{V}_k \in \mathbb{C}^{N_r \times N_s}$. Then, the received signal $\mathbf{y}_k$ at the *k*-th GT is formulated as

$$\begin{aligned} \mathbf{y}_k &= \boldsymbol{V}_k^H \tilde{\boldsymbol{H}}_k \boldsymbol{S} \boldsymbol{W} \boldsymbol{c} + \boldsymbol{V}_k^H \boldsymbol{n}_k \\ &= (d_k)^{-\frac{\alpha}{2}} \boldsymbol{V}_k^H \boldsymbol{H}_k \boldsymbol{S} \boldsymbol{W} \boldsymbol{c} + \boldsymbol{V}_k^H \boldsymbol{n}_k, \end{aligned} \quad (5)$$

where $\boldsymbol{W} = [\boldsymbol{W}_1, \boldsymbol{W}_2, \ldots, \boldsymbol{W}_K] \in \mathbb{C}^{N_t^{RF} \times K N_s}$ is the digital precoder and $\boldsymbol{W}_k \in \mathbb{C}^{N_t^{RF} \times N_s}$, $1 \leq k \leq K$ denotes the digital precoder for the *k*-th GT, $\boldsymbol{c} = [\boldsymbol{c}_1^T, \boldsymbol{c}_2^T, \ldots, \boldsymbol{c}_K^T]^T \in \mathbb{C}^{K N_s \times 1}$ denotes the transmitted signal vector for K GTs with normalized power $\mathbb{E}(\boldsymbol{c}\boldsymbol{c}^T) = \boldsymbol{I}$. $\boldsymbol{n}_k \sim \mathcal{CN}(0, \sigma^2 \boldsymbol{I}_k)$ is additive white Gaussian noise (AWGN) and the element $s_{i,j}$ of beam selection $\boldsymbol{S} \in \mathbb{C}^{N_t \times N_t^{RF}}$ is set to either 0 or 1. It implies that each column of beam selector has one and only one non-zero element "1".

B. Joint Optimization Problem Formulation

Before proceeding with the detailed derivation analysis, an equivalent $(d_k)^{-\frac{\alpha}{2}}$ is reformulated to make a model mathematically more tractable, which can be rewritten as $(d_k)^{-\frac{\alpha}{2}} = (h^2 + \|\mathbf{z} - \mathbf{x}_k\|_2^2)^{-\frac{\alpha}{2}} = (h^2 + (h\mathbf{tan}\Theta)^2)^{-\frac{\alpha}{2}} = (h\mathbf{sec}\Theta)^{-\alpha}$. Thus, the received signal of GT *k* can be simplified as

$$\mathbf{y}_k = (h\mathbf{sec}\Theta)^{-\alpha} \boldsymbol{V}_k^H \boldsymbol{H}_k \boldsymbol{S} \boldsymbol{W} \boldsymbol{c} + \boldsymbol{V}_k^H \boldsymbol{n}_k. \quad (6)$$

Under the independence assumption of $\{\boldsymbol{c}_k, \boldsymbol{n}_k | k = 1, \ldots, K\}$, we can obtain the well-known MMSE combining matrix $\boldsymbol{V}_k$ by minimizing the MMSE, which is formulated as

$$\begin{aligned} \boldsymbol{V}_k = (h\mathbf{sec}\Theta)^{\alpha} \big(& \boldsymbol{H}_k \boldsymbol{S} \boldsymbol{W} \boldsymbol{W}^H \boldsymbol{S}^H \boldsymbol{H}_k^H \\ & + \sigma^2 (h\mathbf{sec}\Theta)^{2\alpha} \boldsymbol{I}_{N_r} \big)^{-1} \boldsymbol{H}_k \boldsymbol{S} \boldsymbol{W}. \end{aligned} \quad (7)$$

According to (6), the hybrid precoder optimization problem is designed by assuming the combining matrix is used in (7). Thus, the proposed joint optimization problem is to maximize the spectral efficiency (SE) of the downlink system, which is formulated as

$$\max_{\boldsymbol{W}, \boldsymbol{S}, h} \sum_{k=1}^{K} \log \det \left(\boldsymbol{I}_{N_r} + \frac{\boldsymbol{H}_k \boldsymbol{S} \boldsymbol{W} \boldsymbol{W}^H \boldsymbol{S}^H \boldsymbol{H}_k^H}{\sigma^2 (h\mathbf{sec}\Theta)^{2\alpha}} \right) \quad (8a)$$

$$s.t. \ \ \mathrm{tr}\left(\boldsymbol{W}^H \boldsymbol{S}^H \boldsymbol{S} \boldsymbol{W} \right) \leq P, \quad (8b)$$

$$\sum_{i=1}^{N_t} s_{i,j} = 1, \quad \sum_{j=1}^{N_t^{RF}} s_{i,j} \leq 1, \quad s_{i,j} \in \{0, 1\}, \quad (8c)$$

$$h_{\min} \leq h \leq h_{\max}, \quad (8d)$$

$$(7), \quad (8e)$$

where P is the total transmit power at the BS. Due to the effect of obstacle height and authority regulations of UAVs, the feasible region of height h is determined as $[h_{\min}, h_{\max}]$. The constraints $\sum_{j=1}^{N_r^{RF}} s_{i,j} \leq 1, i = 1, 2, ..., N_t$ guarantee that each beam is selected for at most one RF chain, while the constraints $\sum_{i=1}^{N_t} s_{i,j} = 1, j = 1, 2, ..., N_r^{RF}$ ensure that each beam is generated by a single RF chain.

It is worth mentioning that the optimization problem (8) involves joint optimization over three variables along with non-convex constraints, which is difficult to solve straightforwardly. Furthermore, the fixed combining matrix would lead to the performance reducing. To solve above issues, the equivalent optimization problem is proposed that transforms the problem (8) into a more tractable form. Firstly, MSE is introduced as the objective function for the joint altitude of UAV, the beam selection and transmit/receive precoding design, which can be expressed as $\boldsymbol{E}_k = \mathbb{E}\{(\mathbf{y}_k - \boldsymbol{c}_k)(\mathbf{y}_k - \boldsymbol{c}_k)^H\}$ [44]. Moreover, since $\mathbf{y}_k$ and $\boldsymbol{n}_k$ are mutually independent, $\boldsymbol{E}_k$ can be further expressed as

$$\begin{aligned} \boldsymbol{E}_k = & (h\mathbf{sec}\Theta)^{-2\alpha} \boldsymbol{V}_k^H \boldsymbol{H}_k \boldsymbol{S} \boldsymbol{W} \boldsymbol{W}^H \boldsymbol{S}^H \boldsymbol{H}_k^H \boldsymbol{V}_k \\ & - 2(h\mathbf{sec}\Theta)^{-\alpha} \mathfrak{Re}\left(\boldsymbol{V}_k^H \boldsymbol{H}_k \boldsymbol{S} \boldsymbol{W} \right) + \sigma^2 \boldsymbol{V}_k^H \boldsymbol{V}_k + I_{N_s}. \end{aligned} \quad (9)$$

By introducing auxiliary weighting matrices ξ_k, the sum-rate maximization problem (8) is equivalently expressed as follows

$$\min_{\boldsymbol{W},\boldsymbol{V}_k^H,\boldsymbol{S},h,\xi_k} \sum_{k=1}^{K} \left(\log\det(\xi_k) - \mathrm{tr}(\xi_k \boldsymbol{E}_k) + N_s\right) \tag{10a}$$

$$s.t. \quad \mathrm{tr}\left(\boldsymbol{W}^H \boldsymbol{S}^H \boldsymbol{S} \boldsymbol{W}\right) \le P, \tag{10b}$$

$$\sum_{j=1}^{N_t^{RF}} s_{i,j} \le 1, \quad \sum_{i=1}^{N_t} s_{i,j} = 1, \quad s_{i,j} \in \{0,1\}, \tag{10c}$$

$$h_{\min} \le h \le h_{\max}, \tag{10d}$$

where ξ_k is obtained by $\boldsymbol{E}_k^{-1}$.

Proof: The proof is given in Appendix.

Instead of the original optimization problem (8), a more tractable minimum weighted mean squared error (MWMSE) optimization problem (10) is considered. For this kind of combinatorial optimization problem, the optimal digital combiner for each GT are separable, and can be estimated independently. Therefore, the optimization problem (10) can be decomposed as the subproblems $\boldsymbol{V}_k^H = \arg\min_{\boldsymbol{V}_k^H} \boldsymbol{E}_k$ for $k = 1, 2, \ldots, K$. Considering the partial derivative of (10a) with respect to $\boldsymbol{V}_k^H$ and ignoring the constant term ξ_k, we have

$$\boldsymbol{V}_k^H = \boldsymbol{W}_k^H \overline{\boldsymbol{H}}_k^H \left(\overline{\boldsymbol{H}}_k \boldsymbol{W} \boldsymbol{W}^H \overline{\boldsymbol{H}}_k^H + \sigma^2 \boldsymbol{I}_{N_r}\right)^{-1}, \tag{11}$$

where $\overline{\boldsymbol{H}}_k = (h\mathbf{sec}\Theta)^{-\alpha} \boldsymbol{H}_k \boldsymbol{S}$.

For the digital precoder $\boldsymbol{W}$ at the UAV, the MSE of K GTs is considered, i.e.,$\boldsymbol{E} = \sum_{k=1}^{K} \boldsymbol{E}_k$. Similar to (9), $\boldsymbol{E}$ can be expressed as

$$\begin{aligned}\boldsymbol{E} = {} & \mathrm{tr}\left(\boldsymbol{V}^H \overline{\boldsymbol{H}} \boldsymbol{W} \boldsymbol{W}^H \overline{\boldsymbol{H}}^H \boldsymbol{V}\right) - \mathrm{tr}\left(\boldsymbol{V}^H \overline{\boldsymbol{H}} \boldsymbol{W}\right) \\ & + \boldsymbol{\sigma}^2 \mathrm{tr}\left(\boldsymbol{V}^H \boldsymbol{V}\right) - \mathrm{tr}\left(\boldsymbol{W}^H \overline{\boldsymbol{H}}^H \boldsymbol{V}\right) + K N_s. \end{aligned} \tag{12}$$

where $\overline{\boldsymbol{H}} = [\overline{\boldsymbol{H}}_1, \overline{\boldsymbol{H}}_2, .., \overline{\boldsymbol{H}}_K]^T$, $\boldsymbol{V} = \mathrm{diag}(\boldsymbol{V}_1, \boldsymbol{V}_2, .., \boldsymbol{V}_K)$ represents the digital combiner for K GTs. According to the Karush-Kuhn-Tucker (KKT) condition, the optimal solution of $\boldsymbol{W}$ can be solved by the following closed form

$$\boldsymbol{W} = \left(\overline{\boldsymbol{H}}^H \boldsymbol{V} \boldsymbol{V}^H \overline{\boldsymbol{H}}\right)^{-1} \overline{\boldsymbol{H}}^H \boldsymbol{V}. \tag{13}$$

From (11) and (13), it can observe that the solutions of $\boldsymbol{V}_k^H$ and $\boldsymbol{W}$ depend on each other. To solve this optimization problem, the classical BCD algorithm is usually used to divide the MWMSE optimization problem into a sequence of sub-problems, and optimize each variable separately. However, when different variables in problem (10) are coupling constraints for each other, the BCD algorithm cannot be directly performed. To tackle the coupling constraint, the penalty function method will be introduced to solve the minimization problem (10). Next, the BCD algorithm with penalty function is proposed to solve the each of subproblems.

III. Proposed Hybrid Precoding Design

The main efforts of this section is solve the optimization problem (10) by exploiting BCD algorithm based on the augmented Lagrangian method. Note that the transmit precoder and receive combiners are coupled with each other in the power constraint, which is difficult to achieve the optimal solution. To this end, the original problem is divided into a series of sub-problems: weighting matrices ξ_k, altitude of UAV h, digital combiners $\boldsymbol{V}_k^H$, digital precoder $\boldsymbol{W}$, beam selector $\boldsymbol{S}$ and solving each independently. The specific procedures are summarized as follows.

A. Optimization of the Weighting Matrices ξ_k

Under fixed variables $\boldsymbol{W}$, $\boldsymbol{V}_k^H$, $\boldsymbol{S}$ and h, the optimization problem (10) with respect to ξ_k is rewritten as

$$\min_{\xi_k} \sum_{k=1}^{K} \log\det(\xi_k) - \mathrm{tr}(\xi_k \boldsymbol{E}_k). \tag{14}$$

By taking the derivative of the optimization problem (14) with respect to ξ_k to zero. Thus, the optimal ξ_k^* can be obtained as

$$\begin{aligned}\xi_k^* = \boldsymbol{E}_k^{-1} = {} & [(h\mathbf{sec}\Theta)^{-2\alpha} \boldsymbol{V}_k^H \boldsymbol{H}_k \boldsymbol{S} \boldsymbol{W} \boldsymbol{W}^H \boldsymbol{S}^H \boldsymbol{H}_k^H \boldsymbol{V}_k \\ & - 2(h\mathbf{sec}\Theta)^{-\alpha} \mathfrak{Re}\left(\boldsymbol{V}_k^H \boldsymbol{H}_k \boldsymbol{S} \boldsymbol{W}\right) + \sigma^2 \boldsymbol{V}_k^H \boldsymbol{V}_k + \boldsymbol{I}_{N_s}]^{-1}. \end{aligned} \tag{15}$$

B. Optimization of the Altitude H

We investigate the altitude planning of UAV with fixed ξ_k, $\boldsymbol{W}$, $\boldsymbol{V}_k^H$ and $\boldsymbol{S}$. Then, the optimization problem (10) with respect to h is formulated as

$$\min_{h} \sum_{k=1}^{K} (h\mathbf{sec}\Theta)^{-2\alpha} A_k - (h\mathbf{sec}\Theta)^{-\alpha} B_k + C_k, \tag{16a}$$

$$s.t. \quad h_{\min} \le h \le h_{\max}, \tag{16b}$$

where $A_k = \mathrm{tr}(\xi_k \boldsymbol{V}_k^H \boldsymbol{H}_k \boldsymbol{S} \boldsymbol{W} \boldsymbol{W}^H \boldsymbol{S}^H \boldsymbol{H}_k^H \boldsymbol{V}_k)$, $B_k = 2\mathrm{tr}(\boldsymbol{V}_k^H \boldsymbol{H}_k \boldsymbol{S} \boldsymbol{W})$, $C_k = [\boldsymbol{\sigma}^2 \mathrm{tr}(\xi_k \boldsymbol{V}_k^H \boldsymbol{V}_k) + \xi_k \boldsymbol{I}_{N_s}]$.

Based on (16), defining function $f(\mathbf{x}(h)) \triangleq A_k \mathbf{x}^2(h) - B_k \mathbf{x}(h) + C_k$ and $\mathbf{x}(h) \triangleq (h\mathbf{sec}\Theta)^{-\alpha}$, we have

$$f'(\mathbf{x}(h)) = 2A_k x(h) - B_k. \tag{17}$$

It follows that the optimal altitude of UAV is obtained in the following two cases.

1) Case 1: If $x(h) > \frac{B_k}{2A_k}$, we have $f'(\mathbf{x}(h)) > 0$, and $f(\mathbf{x}(h))$ is an increasing function when $h_{\min} \le h \le h_{\max}$. The optimal value of h is denoted by h^*. Then, it is observed that the $\mathbf{x}(h)$ is a monotonic decreasing function with respect to h, which yields

$$h^* = h_{\max}. \tag{18}$$

2) Case 2: If $x(h) \le \frac{B_k}{2A_k}$ and $h_{\min} \le h \le h_{\max}$, $f(\mathbf{x}(h))$ is a monotonically decreasing function. The optimal $\mathbf{x}(h)^*$ is

$$h^* = h_{\min}. \tag{19}$$

After the flight altitude h^* is obtained, a 2D exhaustive search is used to achieve the optimal location planning $\mathbf{x}$ of UAV to the optimization problem (16). Symmetries are an abvious device to cut out portions of the configuration space, which can reduce the size of the search space by a factor of about 1/8 [45]. Thus, 2D exhaustive search with symmetries scheme is considered to reduce the complexity.

C. Optimization of the Beam Selection and Beamspace Precoding Matrix

To tackle the coupling constraint, the framework of the classic penalty dual decomposition (PDD) [46] is adopted to solve the problem (10). Before proceeding to the derivation of the PDD method, the auxiliary variables $\{\hat{s}_{i,j}\}$ and $\boldsymbol{Q}_k$ are introduced, which are subject to the constraints of $s_{i,j} = \hat{s}_{i,j}$, $s_{i,j}(1-\hat{s}_{i,j}) = 0$, $0 \le \hat{s}_{i,j} \le 1$ and $\boldsymbol{Q}_k = \boldsymbol{S}\boldsymbol{W}_k$. Let $s_i^T \in \mathbb{C}^{1\times N_t^{RF}}$ be the i-th row of $\boldsymbol{S}$, the constraint $\sum_{j=1}^{N_r^{RF}} s_{i,j} \le 1$ is redefined as $s_i^T\mathbf{1} \le 1$ and the elements of vector $\mathbf{1} \in \mathbb{C}^{N_t^{RF}\times 1}$ are 1. Furthermore, $s_{i,j}$ is represented as $s_i^T f_j$, where $f_j \in \mathbb{C}^{N_r^{RF}\times 1}$ is the j-th column of $\boldsymbol{I}_{N_r^{RF}}$. According to above notations, the optimization problem (10) is reformulated as follows

$$\min_{\boldsymbol{W}_k,\boldsymbol{V}_k^H,\boldsymbol{Q}_k,\{\hat{s}_{i,j}\}} \sum_{k=1}^{K} \mathrm{tr}\left(\xi_k \boldsymbol{E}_k\right) \tag{20a}$$

$$s.t. \sum_{k=1}^{K} \|\boldsymbol{Q}_k\|_F^2 \le P, \tag{20b}$$

$$\boldsymbol{Q}_k = \boldsymbol{S}\boldsymbol{W}_k, \tag{20c}$$

$$s_i^T f_j(1-\hat{s}_{i,j}) = 0, \quad s_i^T f_j - \hat{s}_{i,j} = 0, \tag{20d}$$

$$\sum_{i=1}^{N_t} s_i^T f_j = 1, \tag{20e}$$

$$s_i^T\mathbf{1} \le 1, \quad 0 \le \hat{s}_{i,j} \le 1, \tag{20f}$$

where $\boldsymbol{E}_k$ is given by

$$\boldsymbol{E}_k = (\boldsymbol{I} - \boldsymbol{V}_k^H\boldsymbol{H}_k\boldsymbol{Q}_k)(\boldsymbol{I} - \boldsymbol{V}_k^H\boldsymbol{H}_k\boldsymbol{Q}_k)^H + \sigma^2\boldsymbol{V}_k^H\boldsymbol{V}_k.$$

It turns out that the minimization problem (20) is still not easy to solve. For this purpose, the above constraint minimization problem is transformed into an unconstrained one by adopting the penalty function. The multiplier variables $\{\boldsymbol{L}_k\}$ is introduced for the constraints $\{\boldsymbol{Q}_k = \boldsymbol{S}\boldsymbol{W}_k\}$ and the problem (20) is given by

$$\begin{aligned}
&\min_{\boldsymbol{W}_k,\boldsymbol{V}_k^H,\boldsymbol{Q}_k,\{\hat{s}_{i,j}\},s_j} \sum_{k=1}^{K} \mathrm{tr}\left(\xi_k \boldsymbol{E}_k\right) \\
&\quad + \frac{1}{2\rho}\sum_{k=1}^{K} \|\boldsymbol{Q}_k - \boldsymbol{S}\boldsymbol{W}_k + \rho\boldsymbol{L}_k\|_F^2 \\
&\quad + \frac{1}{2\rho}\sum_{j=1}^{N_t^{RF}} \left(\sum_{i=1}^{N_t} s_i^T f_j - 1 + \rho\mu_j\right)^2 \\
&\quad + \frac{1}{2\rho}\sum_{i=1}^{N_t}\sum_{j=1}^{N_t^{RF}} \left(s_i^T f_j(1-\hat{s}_{i,j}) + (s_i^T f_j - \hat{s}_{i,j}) + \rho\lambda_{i,j}\right)^2, \\
&\qquad s.t. \sum_{k=1}^{K} \|\boldsymbol{Q}_k\|_F^2 \le P, \\
&\qquad\quad s_i^T\mathbf{1} \le 1, \quad 0 \le \hat{s}_{i,j} \le 1,
\end{aligned} \tag{21}$$

where ρ is the scalar penalty parameter, $\lambda_{i,j}$ and μ_j are Lagrangian multipliers corresponding to the minimum rate constraints.

In the following, we focus on solving the corresponding optimization problem (21) by exploiting BCD type algorithm. The optimization variables are divided into a number of blocks variables $\boldsymbol{W}_k, \boldsymbol{V}_k^H, \boldsymbol{Q}_k$ and $\boldsymbol{S}$, such that for each block the corresponding subproblem can be solved independently. Specifically, the details about the process of each subproblems are given as follows.

1) The Subproblem $\{\boldsymbol{V}_k^H\}$: We optimize the variables $\boldsymbol{V}_k^H$ with fixing the other variables. The $\boldsymbol{V}_k^H$ is optimized through the following problem

$$\min_{\boldsymbol{V}_k^H} \sum_{k=1}^{K} \mathrm{tr}\left(\xi_k \boldsymbol{E}_k\right). \tag{22}$$

And then, using the KKT condition of (22) with respect to $\boldsymbol{V}_k^H$, the optimal $\boldsymbol{V}_k$ can be derived as a function of $\boldsymbol{Q}_k$ as follows

$$\boldsymbol{V}_k^H = (h\mathbf{sec}\Theta)^{\alpha}\boldsymbol{Q}_k^H\boldsymbol{H}_k^H\left(\boldsymbol{H}_k\boldsymbol{Q}_k\boldsymbol{Q}_k^H\boldsymbol{H}_k^H + \sigma^2(h\mathbf{sec}\Theta)^{2\alpha}\boldsymbol{I}\right)^{-1}. \tag{23}$$

2) The Subproblem w.r.t. $\boldsymbol{W}_k$: The optimized $\boldsymbol{W}_k$ is achieved by solving the following minimization problem

$$\min_{\boldsymbol{W}_k} \|\boldsymbol{Q}_k - \boldsymbol{S}\boldsymbol{W}_k + \rho\boldsymbol{L}_k\|_F^2. \tag{24}$$

Similarly, the optimal $\boldsymbol{W}_k$ can be obtained by exploiting the optimality conditions of first order in (24), which yields

$$\boldsymbol{W}_k = \left(\boldsymbol{S}^H\boldsymbol{S}\right)^{-1}\boldsymbol{S}^H\left(\boldsymbol{Q}_k - \rho\boldsymbol{L}_k\right). \tag{25}$$

3) The Subproblem w.r.t. $\{\boldsymbol{Q}_k\}$: The subproblems of optimizing $\{\boldsymbol{Q}_k\}$ are updated by solving the following minimization problem

$$\begin{aligned}
&\min_{\boldsymbol{Q}_k} \sum_{k=1}^{K}\left\{\mathrm{tr}\left(\xi_k\boldsymbol{E}_k\right) + \frac{1}{\rho}\|\boldsymbol{Q}_k - \boldsymbol{S}\boldsymbol{W}_k + \rho\boldsymbol{L}_k\|_F^2\right\} \\
&\qquad s.t. \quad \sum_{k=1}^{K}\|\boldsymbol{Q}_k\|_F^2 \le P.
\end{aligned} \tag{26}$$

By expanding $\|\boldsymbol{Q}_k - \boldsymbol{S}\boldsymbol{W}_k + \rho\boldsymbol{L}_k\|_F^2$ and some appropriate rearrangement, the minimization problem (26) can be equivalently rewritten as

$$\begin{aligned}
&\min_{\boldsymbol{Q}_k} \sum_{k=1}^{K}\left\{\mathrm{tr}\left(\xi_k\boldsymbol{E}_k\right) + \frac{1}{\rho}\mathrm{tr}\left(\boldsymbol{Q}_k^H\boldsymbol{Q}_k\right) - \frac{2}{\rho}\mathfrak{Re}\left\{\mathrm{tr}\left(\boldsymbol{Q}_k^H\boldsymbol{B}_k\right)\right\}\right\} \\
&\qquad s.t. \quad \sum_{k=1}^{K}\|\boldsymbol{Q}_k\|_F^2 \le P,
\end{aligned} \tag{27}$$

where $\boldsymbol{B}_k$ is introduced for simplicity and given by $\boldsymbol{B}_k = (\boldsymbol{S}\boldsymbol{W}_k - \rho\boldsymbol{L}_k)$.

The above problem (27) is a convex quadratic optimization problem, which can be solved successively according to the Lagrangian function. By attaching a Lagrange multiplier $\eta \ge 0$,

the closed-form solution of the optimal $\boldsymbol{Q}_k$ is given by

$$\boldsymbol{Q}_k = \left(\boldsymbol{I} + \rho\eta\boldsymbol{I} + \rho\boldsymbol{H}_k^H\boldsymbol{V}_k\xi_k\boldsymbol{V}_k^H\boldsymbol{H}_k\right)^{-1}\left(\boldsymbol{B}_k + 2\rho\boldsymbol{H}_k^H\boldsymbol{V}_k\xi_k\right). \tag{28}$$

where η is chosen by using bisection method.

4) The Subproblem w.r.t. $\{\hat{s}_{i,j}\}$*:* The variable $\{\hat{s}_{i,j}\}$ is updated by fixing the remaining variables. The minimization subproblem with respect to $\{\hat{s}_{i,j}\}$ can be rewritten as

$$\min_{\hat{s}_{i,j}} \frac{1}{2\rho}\left(s_i^T f_j(1-\hat{s}_{i,j}) + (s_i^T f_j - \hat{s}_{i,j}) + \rho\lambda_{i,j}\right)^2 \tag{29a}$$

$$s.t. \quad 0 \le \hat{s}_{i,j} \le 1. \tag{29b}$$

It is not difficult to find that the (29a) is a scalar continuously differentiable function. By enforcing the KKT condition, the optimization problem (29a) can be solved by

$$\hat{s}_{i,j} = \frac{2s_{i,j}^2 + (2+\rho\lambda_{i,j})s_{i,j} + \rho\lambda_{i,j}}{(1+s_{i,j})^2}. \tag{30}$$

Recalling that $\hat{s}_{i,j}$ satisfies $0 \le \hat{s}_{i,j} \le 1$, the solution of the constrained problem (29) is easily given by

$$s_{i,j}^* = \begin{cases} 1, & 1 \le \hat{s}_{i,j}, \\ \hat{s}_{i,j}, & 0 < \hat{s}_{i,j} < 1, \\ 0, & \hat{s}_{i,j} \le 0. \end{cases} \tag{31}$$

5) The Subproblem w.r.t. $\{\mathbf{s}_i\}$*:* The subproblem of optimizing $\{s_i\}$ can be updated by introducing the Lagrange multiplier, which yields

$$\begin{aligned} \min_{s_i} & \frac{1}{2\rho}\sum_{j=1}^{N_t^{RF}}\left(\sum_{i=1}^{N_t} s_i^T f_j - 1 + \rho\mu_j\right)^2 \\ & + \frac{1}{2\rho}\sum_{i=1}^{N_t}\sum_{j=1}^{N_t^{RF}}\left(s_i^T f_j(1-\hat{s}_{i,j}) + (s_i^T f_j - \hat{s}_{i,j}) + \rho\lambda_{i,j}\right)^2 \\ s.t. \quad & s_i^T\mathbf{1} \le 1,\ i = 1, 2, \ldots, N_t. \end{aligned} \tag{32}$$

It is clear that the optimization problem (32) associated with each s_i are convex. By examining the KKT optimality condition, the closed-form solution of optimization problem (32) with respect to s_i yields:

$$\begin{aligned} s_i = & \left(3\boldsymbol{I} + \sum_{j=1}^{N_t^{RF}}(\hat{s}_{i,j}^2 - 2\hat{s}_{i,j})f_j f_j^T\right)^{-1} \\ & \times \left(\sum_{j=1}^{N_t^{RF}}\left(\rho\lambda_{i,j}(1-\hat{s}_{i,j}) + (\sum_{k=i}^{N_t} s_k^T f_j + \rho\mu_j - 1)\right)f_j\right). \end{aligned} \tag{33}$$

Finally, the beam selector $\boldsymbol{S}$ can be solved by using the one-iteration BCD method, which is summarized in Algorithm 1. The remaining task is to update $\{\boldsymbol{L}_k\}$, $\{\lambda_{i,j}\}$, $\{\mu_j\}$ and ρ. The multiplier variables $\{\boldsymbol{L}_k\}$, $\{\lambda_{i,j}\}$ and $\{\mu_j\}$ are updated as follows

$$\boldsymbol{L}_k^{(n+1)} = \boldsymbol{L}_k^{(n)} + \frac{1}{\rho^{(n)}}\left(\boldsymbol{Q}_k - \boldsymbol{S}\boldsymbol{W}_k\right), \tag{34a}$$

Algorithm 1: Solving (32) by BCD Algorithm.

1: **For**: $i = 1, \ldots, N_t$.
2: Update the s_i according to (33);
3: Assign s_i to the i-th row of $\boldsymbol{S}$;
4: **End For**

Algorithm 2: The Proposed Joint Optimization Algorithm.

1: **Input**: the maximum transmit power P, and channel $\boldsymbol{H}_k$ for $1 \le k \le K$.
2: **Initialization**: $n = 1$, $\mathcal{K} = \{1, 2, \ldots, K\}$, primal variables $\{\boldsymbol{V}_k, \boldsymbol{W}, \overline{\boldsymbol{H}}_k, \boldsymbol{Q}_k, \hat{s}_{i,j}, s_j\}$, initial $h = h_{\max}$, dual variables $\{\boldsymbol{L}_k^{(n)}, \lambda_{i,j}^{(n)}, \mu_j^{(n)}, \rho^{(n)}\}$;
3: **while** termination condition is not reached **do**
4: Update $\{\xi_k\}$ according to (15);
5: Update the altitude h according to (16);
6: Update $\{\boldsymbol{V}_k\}$ according to (23);
7: Update $\boldsymbol{W}$ according to (25);
8: Update $\{\boldsymbol{Q}_k\}$ according to (28);
9: Update $\{\hat{s}_{i,j}\}$ according to (31);
10: Update $\{s_j\}$ according to (33);
11: Update $\{\boldsymbol{L}_k^{(n)}, \lambda_{i,j}^{(n)}, \mu_j^{(n)}, \rho^{(n)}\}$ according to (34) (35);
12: **end while**
13: **Output** analog part $\boldsymbol{S}$ and digital part $\boldsymbol{W}$, $\boldsymbol{V}_k$, h.

$$\lambda_{i,j}^{(n+1)} = \lambda_{i,j}^{(n)} + \frac{1}{\rho^{(n)}}\left(s_i^T f_j(2-\hat{s}_{i,j}) - \hat{s}_{i,j}\right), \tag{34b}$$

$$\mu_j^{(n+1)} = \mu_j^{(n)} + \frac{1}{\rho^{(n)}}\left(\sum_{i=1}^{N_t}(s_i^T\mathbf{1} - 1)\right) \tag{34c}$$

and the penalty parameter ρ is updated as follows

$$\rho^{(n+1)} = \begin{cases} \kappa\rho^{(n)}, & \frac{\left\|\boldsymbol{E}_k^{(n)} - \boldsymbol{E}_k^{(n-1)}\right\|_F^2}{\left\|\boldsymbol{E}_k^{(n-1)} - \boldsymbol{E}_k^{(n-2)}\right\|_F^2} > \varepsilon, \\ \rho^{(n)}, & \text{otherwise}, \end{cases} \tag{35}$$

where $\kappa > 0$, $\varepsilon < 1$ are used to control the penalty parameter ρ. The detailed description for solving the optimization problem (10) is provided in Algorithm 2.

We estimate the computational complexity of the proposed Algorithm 2 by computing the number of required multiplications. The main computational complexity of Algorithm 2 is caused by solving the augmented Lagrange problem (10) which consists of a series of sub-problems, i.e., (14), (16), (22), (24), (27), (29) and (32). The complexities of solving (14) is $\mathcal{O}(N_s^3 + N_r N_s^2)$. The complexities of solving (16) is $\mathcal{O}(N_s^3 + 1.85^K)$. The complexities of solving (22), (24), (27) and (29) are $\mathcal{O}(KN_rN_sN_t^{RF} + N_r^3)$, $\mathcal{O}((N_t^{RF})^2N_t + (N_t^{RF})^3 + KN_tN_sN_t^{RF})$, $\mathcal{O}((N_t^{RF})^3 + (N_t^{RF})^2N_t + N_t^{RF}N_sN_t)$ and $\mathcal{O}(N_tN_t^{RF})$. The complexities of solving (32) is $\mathcal{O}(N_t((N_t^{RF})^2 + (N_t^{RF})^3))$. Therefore, the overall complexity of Algorithm 2 is $\mathcal{O}(I(N_s^3 + N_rN_s^2 + 1.85^K + N_r^2 +$

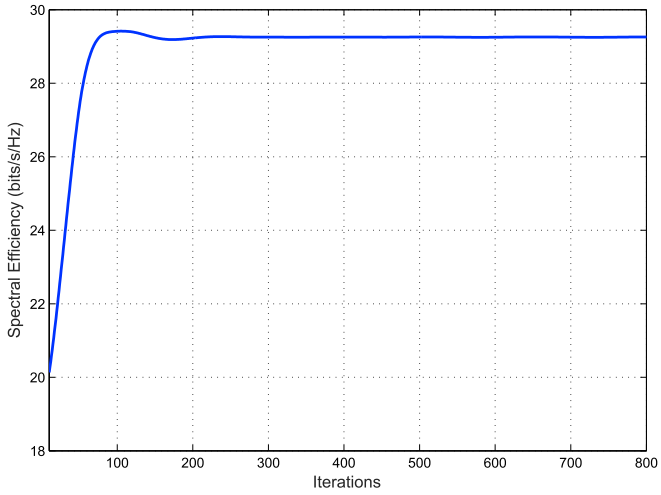

Fig. 3. Achievable SE comparison versus the the number of iterations.

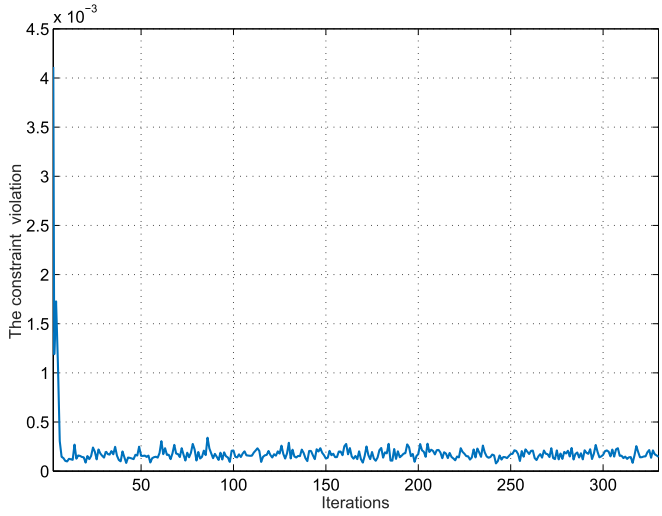

Fig. 4. The constraint violation comparison versus the the number of iterations.

$(N_t^{RF})^2 N_t + N_t (N_t^{RF})^3 + K N_t N_s N_t^{RF} + K N_t N_t^{RF}))$, where I is the numbers of iterations.

Finally, the convergence of Algorithm 2 is considered. The main convergence result is provided in *Theorem 1*.

Theorem 1: Let $\{h, \boldsymbol{V}_{\mathrm{k}}, \boldsymbol{W}, \overline{\boldsymbol{H}}_{\mathrm{k}}, \hat{\mathrm{s}}_{i,j}, \boldsymbol{Q}_{\mathrm{k}}, \mathbf{s}_j, \}$ be the sequence generated by Algorithm 2. If the Robinson $'$ s condition holds for the optimization problem (10). Then, there exists one limit point of sequence of iterations generated by the BCD algorithm, which is a stationary point for the optimization problem (10).

Proof: The detailed proof process of convergence for a general algorithmic framework was provided in [47], [48].

IV. Simulation Results

In this section, simulation results are provided to analyse the effectiveness of the proposed UAV-enabled mmWave MIMO system with the lens antenna arrays. We investigate the SE performance of the proposed UAV-enabled beamspace MIMO scheme and make comparisons with several recent works. Unless specified otherwise, we assume that the UAV is equipped with a DLA to serve $K = 4$ GTs. The antenna number of UAV is $N_t = 64$ and the number of RF chains is $N_t^{RF} = 12$. The GTs are randomly generated and located in the cell of radius of 150 meters. The distance of antenna elements are separated by half of a wavelength. Because of the constraint from the common law, usual practices and conventions, we set the minimum altitude of UAV $h_{\min} = 40$ m and the maximum altitude of UAV $h_{\max} = 120$ m respectively. All simulation results are done in a Monte Carlo fashion with 1000 realizations.

A. Convergence Analysis

The convergence of the proposed algorithm is investigated, as shown in Figs. 3 and 4. From the Fig. 3, it can be observed that after 80 iterations, the value of SE tends to be stable. From these results, we conclude that the proposed algorithm has a rapid convergence. In Fig. 4, we show the value of the constraint violation $\sum_{k=1}^{K} \|\boldsymbol{Q}_k - \overline{\boldsymbol{H}}_k \boldsymbol{W}\|_F^2$ versus the number of iterations for the proposed algorithm. It can be observed that the constraint violation reduces to a threshold $\epsilon = 10^{-4}$, which indicates that the optimal solution has essentially satisfied with the equality constraints (20c) of the optimization problem (20).

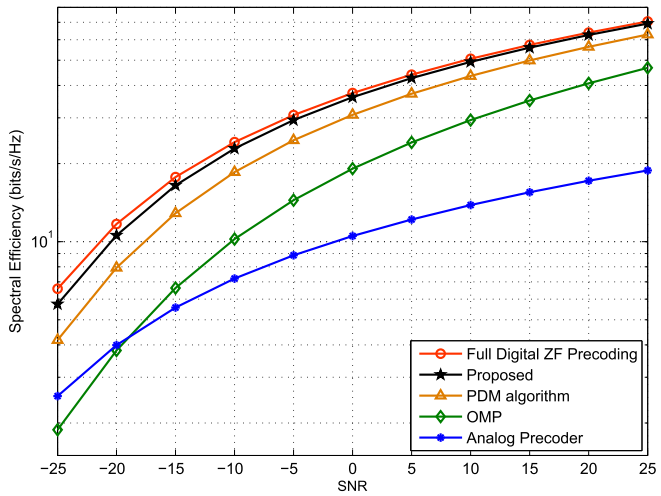

Fig. 5. Achievable SE comparison versus the SNR.

B. Spectral Efficiency Evaluation

Next, the SE achieved by all competing algorithms are investigated, where the number of RF chains and the data streams are set to the same. This is the worst case, since the number of RF chains cannot be smaller than data streams N_s, which also satisfies the constraints in Section II. For comparison, the performance of the full-digital ZF precoding scheme acts as a comparison benchmark precoding scheme (labeled by "FD-ZF"), and we compare the proposed scheme with the PDM [24] and OMP algorithm [49]. As shown in Fig. 5, the existing OMP algorithm achieves a very low SE in all competing methods. On the contrary, the SE of the proposed scheme is quite close to that of the fully digital ZF precoding scheme. This implies that an effective result can be obtained by the proposed scheme to approximate the full digital ZF precoding, even though the RF

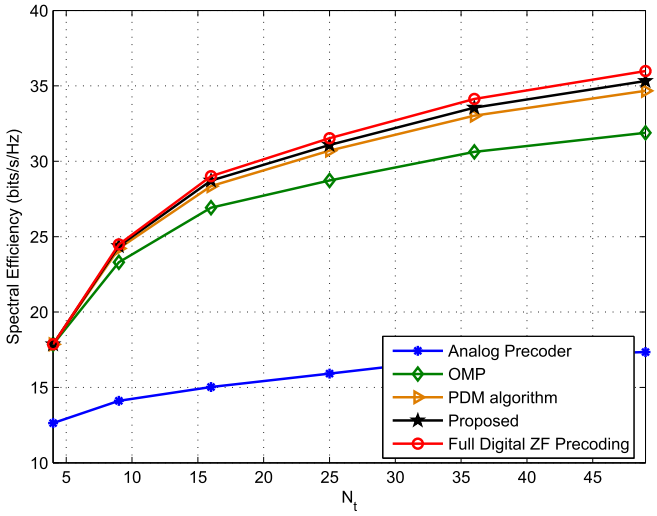

Fig. 6. Achievable SE comparison versus the number of antennas.

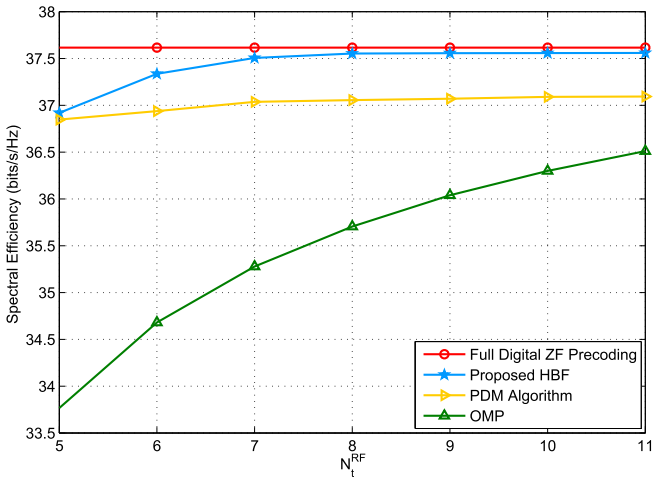

Fig. 7. Achievable SE versus the number of RF chains.

chains are limited. Furthermore, the performance of the analog precoding structures reveals that only using phase shifters will inevitably lead to some non-negligible performance loss.

In Fig. 6, we further analyze the achievable SE comparison for different numbers of antennas. It is shown that when the number of BS antennas N_t grows large, the SE increases without limit, if perfect hardware is assumed while it appears ceilings in practice. It is worth mentioning that when the number of BS antennas is small, the advantage of the proposed scheme is not obvious. In particular, we can observe the OMP, PDM algorithm and the proposed method converge the same SE value with the number of BS antennas $N_t = 4$.

To verify the low hardware cost of the proposed method, the achievable SE of system versus the number of RF chains N_t^{RF} has been shown in Fig. 7, where the number of RF chains N_t^{RF} increases from 5 to 11. It is observed that the performance of all the schemes in general improves with the increase of available RF chains. Interestingly, when the number of N_t^{RF} exceeds 8, the improvement of the proposed scheme is trivial. It is interesting that for all the schemes under consideration, the proposed scheme is equiped with only 6 RF chains to achieve

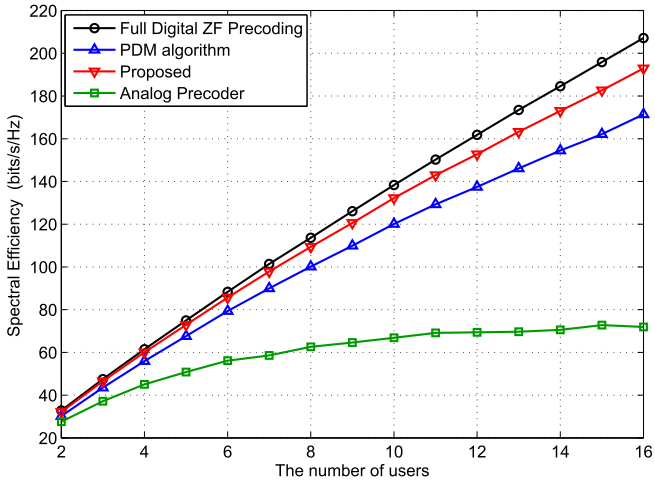

Fig. 8. Achievable SE comparison versus the number of GTs.

over 95 percent of SE in the full digital ZF precoding structure, but other competing methods need more ones.

C. The Performance Evaluation of Different GTs

Finally, we analyze the the achievable SE for the aforementioned schemes versus different numbers of GTs, where the number of GT increases from 2 to 16. In Fig. 8, it can be observed that except the analog precoding scheme, all the other algorithms perform very close to each other under the small number of GTs. The performance of all these schemes increases monotonically with the number of GTs. Besides, the performance gap between the proposed scheme and PDM algorithm would escalate with the increasing number of GTs, which indicates that the proposed scheme has strong potential for large number of GTs scenario.

Fig. 9 illustrates the achievable SE of two existing precoding schemes and the proposed precoding scheme, respectively. It shows that our proposed scheme with LAAs achieves a significant improvement than the conventional analog precoding scheme. Compared to the full digital ZF precoding approach, the proposed precoder have tolerable system performance loss. However, the full digital ZF precoding scheme need more RF chains cost, which is not suitable for compact and lightweight design in UAV-enabled beamspace mmWave MIMO system.

D. The Altitude Optimization of UAV

To verify the necessity of altitude optimization of UAV, we refer the 3GPP specification [50], and the path loss is randomly determined by LoS and NLoS links according to probabilities. Specifically, the probability of the LOS is assumed as (36) shown at the bottom of the next page, and the probability of the NLOS link is given by $P_{NLOS} = 1 - P_{LOS}$. The achievable SE of the proposed scheme versus UAV altitude h is illustrated in Fig. 10, where the h value varies from 40 to 130 m and other parameters are kept unchanged. It can be seen that the achievable SE increases first and then decreases as h increases. This is because that the probability of LoS link between the UAV and GT increases as the UAV height increasing. Therefore, the performance can be improved by increasing the UAV flight

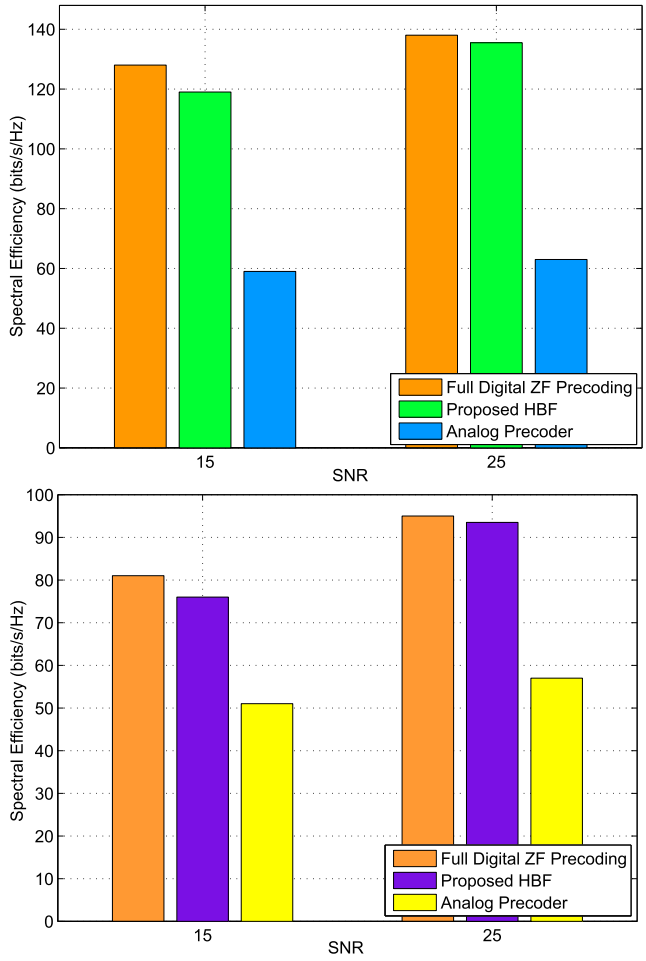

Fig. 9. SE comparison of the analog precoder, fully digital ZF precoder and FD-ZF Precoding (Above: $K = 10$, Below: $K = 6$).

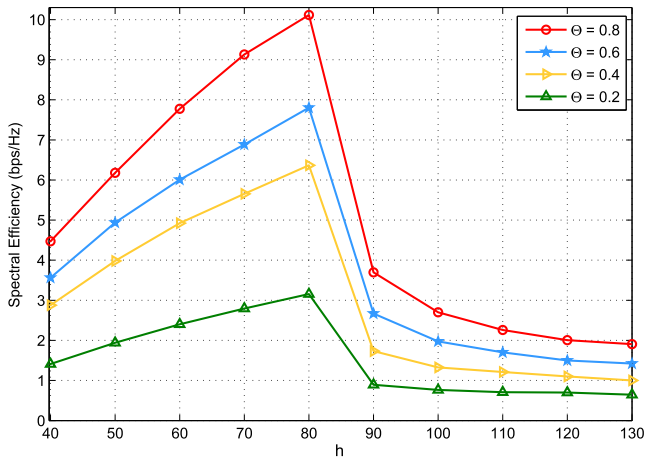

Fig. 10. Achievable SE comparison versus the altitude of UAV h.

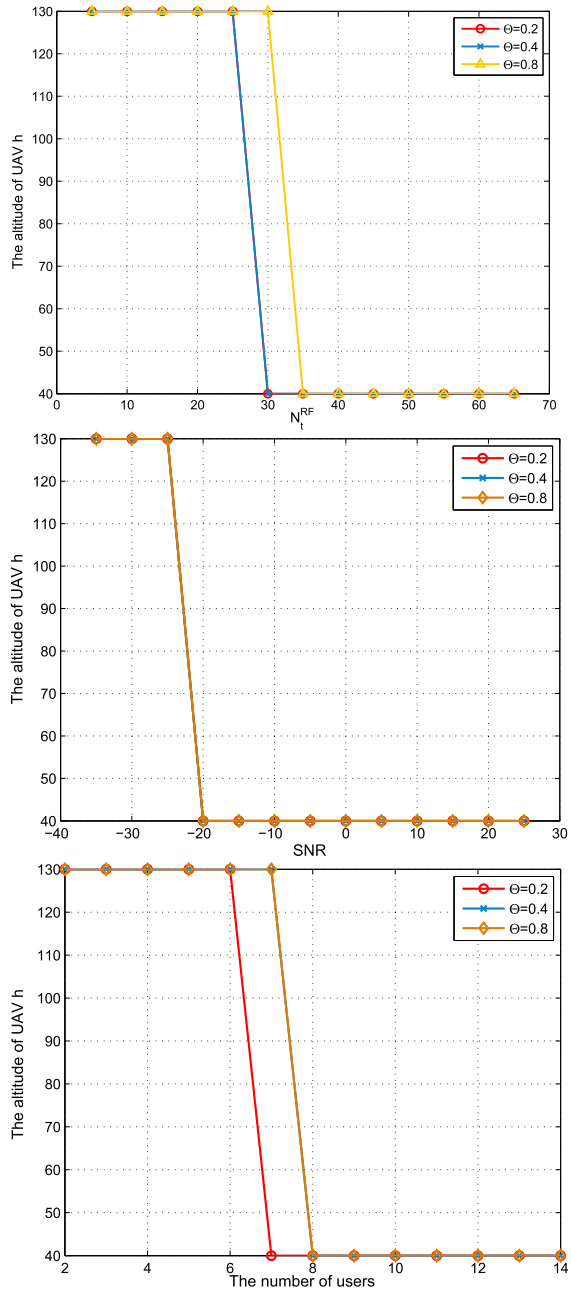

Fig. 11. The altitude of UAV h comparison versus the number of RF chains N_t^{RF}/SNR/users.

altitude within a certain range. However, when the altitude h is sufficiently large, the distance between the UAV and the GT is increasing significantly, which results in high propagation path loss. Therefore, the altitude of UAV needs to be determined

$$P_{LOS} = \begin{cases} 1, & h\sec\Theta \le d_0 \\ \dfrac{d_0}{h\sec\Theta} + \exp\left\{\left(\dfrac{-h\sec\Theta}{\upsilon}\right)\left(1 - \dfrac{d_0}{h\sec\Theta}\right)\right\}, & h\sec\Theta > d_0 \end{cases} \tag{36}$$

reasonably and carefully. To verify this issue, the altitude of UAV versus the number of RF chains/SNR/Users are provided in Fig. 11. The results show that the altitude of UAV h reduces when the number of RF chains/users or SNR value are higher than a threshold value.

V. Conclusion

In this paper, the UAV with LAAs is considered to support multi-user transmission in mmWave beamspace MIMO system. In particular, we focus on jointly optimizing altitude of UAV, transmit precoder, receive combiners as well as beam selector for the sum-rate maximization problem. The original problem is a non-convex, and transmit and receive variables are coupled with each other, which results in extremely strenuous to solve the proposed optimization problem. To solve this limitation, the equivalent optimization problem with the weighted MSE criterion is developed to solve the original non-convex problem. To tackle the coupling constraints problem, an efficient algorithm is proposed based on the principle of alternating optimization, which transforms the original coupling constraints problem into a series of subproblems with separable constraints. Simulation results demonstrate that the proposed algorithm can achieve satisfactory performance and could converge in a few iterations.

Appendix
The Proof of the Problem (10)

Proof: Let $\overline{\boldsymbol{H}}_k = (h\mathbf{sec}\Theta)^{-\alpha}\boldsymbol{H}_k\boldsymbol{S}$ for simplicity. The optimization problem (10) can be rewritten as

$$\min_{\boldsymbol{W},\boldsymbol{V}_k,\boldsymbol{S},\xi_k,h} \sum_{k=1}^{K}\left(\log\det(\xi_k) - \mathrm{tr}(\xi_k\boldsymbol{E}_k) + N_s\right) \tag{37a}$$

$$s.t. \sum_{i=1}^{N_t} s_{i,j} = 1, \quad \sum_{j=1}^{N_r^{RF}} s_{i,j} \le 1, \quad s_{i,j} \in \{0,1\}, \tag{37b}$$

$$h_{\min} \le h \le h_{\max}, \tag{37c}$$

$$(7), \tag{37d}$$

where

$$\boldsymbol{E}_k = \left(\boldsymbol{I}_{N_r} - \boldsymbol{V}_k^H\overline{\boldsymbol{H}}\boldsymbol{W}\right)\left(\boldsymbol{I}_{N_r} - \boldsymbol{V}_k^H\overline{\boldsymbol{H}}\boldsymbol{W}\right)^H + \sigma^2\boldsymbol{V}_k^H\boldsymbol{V}_k.$$

Let $f(\xi_k) = \log\det(\xi_k) - \mathrm{tr}(\xi_k\boldsymbol{E}_k) + N_s$ for simplicity. The optimal ξ_k is updated by taking the derivative of $f(\xi_k)$, we have

$$\frac{\partial\left(\log\det(\xi_k) - \mathrm{tr}(\xi_k\boldsymbol{E}_k)\right)}{\partial\xi_k} = 0. \tag{38}$$

After that, we can obtain the optimal ξ_k as

$$\xi_k^* = \boldsymbol{E}_k^{-1}. \tag{39}$$

Similarly, considering $\overline{\boldsymbol{H}}_k = (h\mathbf{sec}\Theta)^{-\alpha}\boldsymbol{H}_k\boldsymbol{S}$ in (37d), the combining matrix $\boldsymbol{V}_k$ can be rewritten as

$$\boldsymbol{V}_k = (\overline{\boldsymbol{H}}_k\boldsymbol{W}\boldsymbol{W}^H\overline{\boldsymbol{H}}_k^H + \sigma^2\boldsymbol{I}_{N_r})^{-1}\overline{\boldsymbol{H}}_k\boldsymbol{W}. \tag{40}$$

Plugging $\boldsymbol{V}_k$ into (39) yields

$$\xi_k^* = \left(\boldsymbol{I}_{N_r} - \boldsymbol{W}^H\overline{\boldsymbol{H}}_k^H\boldsymbol{J}_k^{-1}\overline{\boldsymbol{H}}_k\boldsymbol{W}\right)^{-1}, \tag{41}$$

where $\boldsymbol{J}_k = \sigma^2\boldsymbol{I}_{N_r} + \overline{\boldsymbol{H}}_k\boldsymbol{W}\boldsymbol{W}^H\overline{\boldsymbol{H}}_k^H$.

Applying the Woodbury matrix identity to (41), $f(\xi_k)$ is recast as

$$\begin{aligned} f(\xi_k) &= \log\det\left(\boldsymbol{E}_k^{-1}\right) - \mathrm{tr}(\xi_k^*\boldsymbol{E}_k) + N_s \\ &= \log\det\left(\boldsymbol{I}_{N_r} - \boldsymbol{W}^H\overline{\boldsymbol{H}}_k^H\boldsymbol{J}_k^{-1}\overline{\boldsymbol{H}}_k\boldsymbol{W}\right)^{-1}. \end{aligned} \tag{42}$$

Thus, we have the following equivalent optimization problem

$$\begin{aligned} \log\det(\xi_k) &= \log\det\left(\left(\boldsymbol{I}_{N_r} - \boldsymbol{W}^H\overline{\boldsymbol{H}}_k^H\boldsymbol{J}^{-1}\overline{\boldsymbol{H}}_k\boldsymbol{W}\right)^{-1}\right) \\ &\overset{(a)}{=} \log\det\left(\boldsymbol{I}_{N_r} + \sigma^{-2}\overline{\boldsymbol{H}}_k\boldsymbol{W}\boldsymbol{W}^H\overline{\boldsymbol{H}}_k^H\right) \\ &\overset{(b)}{=} \log\det\left(\boldsymbol{I}_{N_r} + \frac{\boldsymbol{H}_k\boldsymbol{S}\boldsymbol{W}\boldsymbol{W}^H\boldsymbol{S}^H\boldsymbol{H}_k^H}{\sigma^2(h\mathbf{sec}\Theta)^{2\alpha}}\right), \end{aligned} \tag{43}$$

where (a) is due to the identity $\det(\boldsymbol{I} + \boldsymbol{X}\boldsymbol{Y}) = \det(\boldsymbol{I} + \boldsymbol{Y}\boldsymbol{X})$ and Woodbury matrix identity; (b) is from that $\overline{\boldsymbol{H}}_k = (h\mathbf{sec}\Theta)^{-\alpha}\boldsymbol{H}_k\boldsymbol{S}$. Therefore, the optimization problem (10) is equivalent to the optimization problem (8) and the proof is completed. ■

References

[1] Z. Yang *et al.*, "Joint altitude, beamwidth, location, and bandwidth optimization for UAV-enabled communications," *IEEE Commun. Lett.*, vol. 22, no. 8, pp. 1716–1719, Aug. 2018.

[2] M. Liu, J. Yang, and G. Gui, "DSF-NOMA: UAV-assisted emergency communication technology in a heterogeneous Internet of Things," *IEEE Internet Things J.*, vol. 6, no. 3, pp. 5508–5519, Jun. 2019.

[3] W. Yi, Y. Liu, E. Bodanese, A. Nallanathan, and G. K. Karagiannidis, "A unified spatial framework for UAV-aided mmWave networks," *IEEE Trans. Commun.*, vol. 67, no. 12, pp. 8801–8817, Dec. 2019.

[4] Z. Xiao, P. Xia, and X. Xia, "Enabling UAV cellular with millimeter-wave communication: Potentials and approaches," *IEEE Commun. Mag.*, vol. 54, no. 5, pp. 66–73, May 2016.

[5] P. Yu *et al.*, "Capacity enhancement for 5G networks using mmwave aerial base stations: Self-organizing architecture and approach," *IEEE Wireless Commun.*, vol. 25, no. 4, pp. 58–64, Aug. 2018.

[6] M. T. Dabiri, H. Safi, S. Parsaeefard, and W. Saad, "Analytical channel models for millimeter wave UAV networks under hovering fluctuations," *IEEE Trans. Wireless Commun.*, vol. 19, no. 4, pp. 2868–2883, Apr. 2020.

[7] P. V. Amadori and C. Masouros, "Low RF-complexity millimeter-wave beamspace-MIMO systems by beam selection," *IEEE Trans. Commun.*, vol. 63, no. 6, pp. 2212–2223, Jun. 2015.

[8] Y. Sun and C. Qi, "Weighted sum-rate maximization for analog beamforming and combining in millimeter wave massive MIMO communications," *IEEE Commun. Lett.*, vol. 21, no. 8, pp. 1883–1886, Aug. 2017.

[9] S. Cui, A. J.Goldsmith, and A. Bahai, "Energy-efficiency of MIMO and cooperative MIMO techniques in sensor networks," *IEEE J. Sel. Areas Commun.*, vol. 22, no. 6, pp. 1089–1098, Aug. 2004.

[10] Z. Chen, J. Tang, H. Tang, X. Zhang, D. K. C. So, and K.-K. Wong, "Channel estimation of IRS-aided communication systems with hybrid multiobjective optimization," in *Proc. IEEE Int. Conf. Commun.*, 2021, pp. 1–6.

[11] Z. Chen *et al.*, "Offset learning based channel estimation for intelligent reflecting surface-assisted indoor communication," *IEEE J. Sel. Top. Signal Process.*, be published, doi: 10.1109/JSTSP.2021.3129350.

[12] M. Artuso *et al.*, "Enhancing LTE with Cloud-RAN and load-controlled parasitic antenna arrays," *IEEE Commun. Mag.*, vol. 54, no. 12, pp. 183–191, Dec. 2016.

[13] K. Ntougias, D. K. Ntaikos, C. B. Papadias, and G. K. Papageorgiou, "Coordinated hybrid precoding and QoS-aware power allocation for underlay spectrum sharing with load-controlled antenna arrays," in *Proc. IEEE 20th Int. Workshop Signal Process. Adv. Wireless Commun.*, 2019, pp. 1–5.

[14] B. H. Wang, H. T. Hui, and M. S. Leong, "Global and fast receiver antenna selection for MIMO systems," *IEEE Trans. Commun.*, vol. 58, no. 9, pp. 2505–2510, Sep. 2010.
[15] Y. Gao, H. Vinck, and T. Kaiser, "Massive MIMO antenna selection: Switching architectures, capacity bounds, and optimal antenna selection algorithms," *IEEE Trans. Signal Process.*, vol. 66, no. 5, pp. 1346–1360, Mar. 2018.
[16] W. Shen, X. Bu, X. Gao, C. Xing, and L. Hanzo, "Beamspace precoding and beam selection for wideband millimeter-wave MIMO relying on lens antenna arrays," *IEEE Trans. Signal Process.*, vol. 67, no. 24, pp. 6301–6313, Dec. 2019.
[17] V. V. Ratnam, A. F. Molisch, O. Y. Bursalioglu, and H. C. Papadopoulos, "Hybrid beamforming with selection for multiuser massive MIMO systems," *IEEE Trans. Signal Process.*, vol. 66, no. 15, pp. 4105–4120, Aug. 2018.
[18] M. R. Akdeniz *et al.*, "Millimeter wave channel modeling and cellular capacity evaluation," *IEEE J. Sel. Areas Commun.*, vol. 32, no. 6, pp. 1164–1179, Jun. 2014.
[19] X. Gao, L. Dai, S. Han, C. I, and R. W. Heath, "Energy-efficient hybrid analog and digital precoding for mmwave MIMO systems with large antenna arrays," *IEEE J. Sel. Areas Commun.*, vol. 34, no. 4, pp. 998–1009, Apr. 2016.
[20] J. Zhang, Y. Huang, J. Wang, and L. Yang, "Hybrid precoding for wideband millimeter-wave systems with finite resolution phase shifters," *IEEE Trans. Veh. Technol.*, vol. 67, no. 11, pp. 11285–11290, Nov. 2018.
[21] R. Guo, Y. Cai, M. Zhao, Q. Shi, B. Champagne, and L. Hanzo, "Joint design of beam selection and precoding matrices for mmwave MU-MIMO systems relying on lens antenna arrays," *IEEE J. Sel. Topics Signal Process.*, vol. 12, no. 2, pp. 313–325, May 2018.
[22] R. Méndez-Rial, C. Rusu, N. González-Prelcic, A. Alkhateeb, and R. W. Heath, "Hybrid MIMO architectures for millimeter wave communications: Phase shifters or switches?," *IEEE Access*, vol. 4, pp. 247–267, 2016.
[23] Y. Zeng, R. Zhang, and Z. N. Chen, "Electromagnetic lens-focusing antenna enabled massive MIMO: Performance improvement and cost reduction," *IEEE J. Sel. Areas Commun.*, vol. 32, no. 6, pp. 1194–1206, Jun. 2014.
[24] Y. Zeng and R. Zhang, "Millimeter wave MIMO with lens antenna array: A new path division multiplexing paradigm," *IEEE Trans. Commun.*, vol. 64, no. 4, pp. 1557–1571, Apr. 2016.
[25] T. Xie, L. Dai, D. W. K. Ng, and C. Chae, "On the power leakage problem in millimeter-wave massive MIMO with lens antenna arrays," *IEEE Trans. Signal Process.*, vol. 67, no. 18, pp. 4730–4744, Sep. 2019.
[26] W. Shen, L. Dai, Y. Li, Z. Wang, and L. Hanzo, "Channel feedback codebook design for millimeter-wave massive MIMO systems relying on lens antenna array," *IEEE Wireless Commun. Lett.*, vol. 7, no. 5, pp. 736–739, Oct. 2018.
[27] C. Feng, W. Shen, and J. An, "Beam selection for wideband millimeter wave MIMO relying on lens antenna arrays," *IEEE Commun. Lett.*, vol. 23, no. 10, pp. 1875–1878, Oct. 2019.
[28] X. Yu, J. Zhang, and K. B. Letaief, "A hardware-efficient analog network structure for hybrid precoding in millimeter wave systems," *IEEE J. Sel. Topics Signal Process.*, vol. 12, no. 2, pp. 282–297, May 2018.
[29] X. Gao, L. Dai, Z. Chen, Z. Wang, and Z. Zhang, "Near-optimal beam selection for beamspace mmWave massive MIMO systems," *IEEE Commun. Lett.*, vol. 20, no. 5, pp. 1054–1057, May 2016.
[30] W. Feng, J. Wang, Y. Chen, X. Wang, N. Ge, and J. Lu, "UAV-aided MIMO communications for 5G Internet of Things," *IEEE Internet Things J.*, vol. 6, no. 2, pp. 1731–1740, Apr. 2019.
[31] M. Mozaffari, A. T. Z. Kasgari, W. Saad, M. Bennis, and M. Debbah, "Beyond 5G with UAVs: Foundations of a 3D wireless cellular network," *IEEE Trans. Wireless Commun.*, vol. 18, no. 1, pp. 357–372, Jan. 2019.
[32] H. Huang, Y. Yang, H. Wang, Z. Ding, H. Sari, and F. Adachi, "Deep reinforcement learning for UAV navigation through massive MIMO technique," *IEEE Trans. Veh. Technol.*, vol. 69, no. 1, pp. 1117–1121, Jan. 2020.
[33] C. Liu, K. Ho, and J. Wu, "Mmwave UAV networks with multi-cell association: Performance limit and optimization," *IEEE J. Sel. Areas Commun.*, vol. 37, no. 12, pp. 2814–2831, Dec. 2019.
[34] J. Du, W. Xu, Y. Deng, A. Nallanathan, and L. Vandendorpe, "Energy-saving UAV-assisted multiuser communications with massive MIMO hybrid beamforming," *IEEE Commun. Lett.*, vol. 24, no. 5, pp. 1100–1104, May 2020.
[35] A. Alkhateeb and R. W. Heath, "Frequency selective hybrid precoding for limited feedback millimeter wave systems," *IEEE Trans. Commun.*, vol. 64, no. 5, pp. 1801–1818, May 2016.
[36] Y. Zeng, L. Yang, and R. Zhang, "Multi-user millimeter wave MIMO with full-dimensional lens antenna array," *IEEE Trans. Wireless Commun.*, vol. 17, no. 4, pp. 2800–2814, Apr. 2018.
[37] J. Brady, N. Behdad, and A. M. Sayeed, "Beamspace MIMO for millimeter-wave communications: System architecture, modeling, analysis, and measurements," *IEEE Trans. Antennas Propag.*, vol. 61, no. 7, pp. 3814–3827, Jul. 2013.
[38] A. Sayeed and J. Brady, "Beamspace MIMO for high-dimensional multiuser communication at millimeter-wave frequencies," in *Proc. IEEE Glob. Commun. Conf.*, 2013, pp. 3679–3684.
[39] X. Gao, L. Dai, S. Han, C. I, and X. Wang, "Reliable beamspace channel estimation for millimeter-wave massive MIMO systems with lens antenna array," *IEEE Trans. Wireless Commun.*, vol. 16, no. 9, pp. 6010–6021, Sep. 2017.
[40] H. Li, M. Li, Q. Liu, and A. L. Swindlehurst, "Dynamic hybrid beamforming with low-resolution PSs for wideband mmWave MIMO-OFDM systems," *IEEE J. Sel. Areas Commun.*, vol. 38, no. 9, pp. 2168–2181, Sep. 2020.
[41] Z. Chen, J. Tang, X. Y. Zhang, D. K. C. So, S. Jin, and K.-K. Wong, "Hybrid evolutionary-based sparse channel estimation for IRS-assisted mmwave MIMO systems," *IEEE Trans. Wireless Commun.*, be published, doi: 10.1109/TWC.2021.3105405.
[42] L. Liu, S. Zhang, and R. Zhang, "Multi-beam UAV communication in cellular uplink: Cooperative interference cancellation and sum-rate maximization," *IEEE Trans. Wireless Commun.*, vol. 18, no. 10, pp. 4679–4691, Oct. 2019.
[43] B. Wang, L. Dai, Z. Wang, N. Ge, and S. Zhou, "Spectrum and energy-efficient beamspace MIMO-NOMA for millimeter-wave communications using lens antenna array," *IEEE J. Sel. Areas Commun.*, vol. 35, no. 10, pp. 2370–2382, Oct. 2017.
[44] J. Joung and Y. H. Lee, "Regularized channel diagonalization for multiuser MIMO downlink using a modified MMSE criterion," *IEEE Trans. Signal Process.*, vol. 55, no. 4, pp. 1573–1579, Apr. 2007.
[45] S. Mertens, "Exhaustive search for low-autocorrelation binary sequences," *J. Phys. A: Math. Gen.*, vol. 29, no. 18, pp. 54–73, 1996.
[46] Q. Shi, M. Razaviyayn, Z. Luo, and C. He, "An iteratively weighted MMSE approach to distributed sum-utility maximization for a MIMO interfering broadcast channel," *IEEE Trans. Signal Process.*, vol. 59, no. 9, pp. 4331–4340, Sep. 2011.
[47] Q. Shi and M. Hong, "Penalty dual decomposition method with application in signal processing," in *Proc. IEEE Int. Conf. Acoust., Speech Signal Process.*, 2017, pp. 4059–4063.
[48] Q. Shi and M. Hong, "Penalty dual decomposition method for nonsmooth nonconvex optimization-Part I: Algorithms and convergence analysis," *IEEE Trans. Signal Process.*, vol. 68, pp. 4108–4122, Jun. 2020.
[49] O. E. Ayach, S. Rajagopal, S. Abu-Surra, Z. Pi, and R. W. Heath, "Spatially sparse precoding in millimeter wave MIMO systems," *IEEE Trans. Wireless Commun.*, vol. 13, no. 3, pp. 1499–1513, Mar. 2014.
[50] 3GPP TS 36.777, "Study on enhanced LTE support for aerial vehicles," 3G PP Standard Release 15, pp. 24–29, 2017.

Zhen Chen (Member, IEEE) received the M.S. degree in software engineering from Xiamen University, Xiamen, China, in 2012, and the Ph.D. degree in electronic engineering from the South China University of Technology, Guangzhou, China, in 2019. From 2020 to 2022, he was a Research Fellow with Hong Kong Applied Science and Technology Research Institute, Hong Kong. He is currently a Research Associate with the South China University of Technology.

His current research interests include compressed sensing, reconfigurable intelligent surface, medical image processing, channel estimation, NOMA, beyond 5G and 6G networks. He was the co-recipient of the EAI AICON 2021 best paper awards. He was the exemplary reviewer of several journals.

Nan Zhao (Senior Member, IEEE) is currently a Professor with the Dalian University of Technology, Dalian, China, and the Ph.D. degree in information and communication engineering from the Harbin Institute of Technology, Harbin, China, in 2011. He is on the Editorial Boards of the IEEE WIRELESS COMMUNICATIONS and IEEE WIRELESS COMMUNICATIONS LETTERS. He won the best paper awards in IEEE VTC 2017 Spring, ICNC 2018, WCSP 2018, and WCSP 2019. He was also the recipient of the IEEE Communications Society Asia Pacific Board Outstanding Young Researcher Award in 2018.

Daniel Ka Chun So (Senior Member, IEEE) received the B.Eng. (Hons.) degree in electrical and electronics engineering from The University of Auckland, Auckland, New Zealand, and the Ph.D. degree in electrical and electronics engineering from the Hong Kong University of Science and Technology, Hong Kong. In 2003, he joined the University of Manchester, Manchester, U.K., as a Lecturer, and is currently a Professor and the Discipline Head of Education with the Department of Electrical and Electronic Engineering.

His research interests include green communications, NOMA, beyond 5G and 6G networks, heterogeneous networks, SWIPT, massive MIMO, cognitive radio, D2D and cooperative communications, channel equalization, and estimation techniques. He is currently a Senior Editor of the IEEE WIRELESS COMMUNICATION LETTERS after being the Editor from 2016 to 2020, and the Editor of the IEEE TRANSACTIONS ON WIRELESS COMMUNICATIONS. He is the Lead Guest Editor of the Special Issue in IEEE TRANSACTIONS ON GREEN COMMUNICATIONS AND NETWORKING in 2021. He was also a Symposium Co-Chair of IEEE ICC 2019 and Globecom 2020, and Track Co-Chair of IEEE Vehicular Technology Conference (VTC) Spring 2016, 2017, 2018, 2021, and 2022. He is also the current Chair of the Special Interest Group on Green Cellular Networks within the IEEE ComSoc Green Communications and Computing Technical Committee.

Jie Tang (Senior Member, IEEE) received the B.Eng. degree from the South China University of Technology, Guangzhou, China, the M.Sc. degree from the University of Bristol, Bristol, U.K., and the Ph.D. degree from Loughborough University, Loughborough, U.K. From 2013 to 2015, he was a Research Associate with the School of Electrical and Electronic Engineering, University of Manchester, Manchester, U.K. He is currently a Professor with the School of Electronic and Information Engineering, South China University of Technology.

His current research interests include SWIPT, UAV communications, NOMA, and reconfigurable intelligent surface. He is currently the Editor of the IEEE WIRELESS COMMUNICATIONS LETTERS, IEEE SYSTEMS JOURNAL, and IEEE ACCESS. He is the Guest Editor of the Two Special Issues in IEEE TRANSACTIONS ON GREEN COMMUNICATIONS AND NETWORKING, and One Special Issue in IEEE Open Journal of the Communications Society. He was also a Track Co-Chair of IEEE VTC-Spring 2018, Symposium Co-Chair of IEEE/CIC ICCC 2020, IEEE ComComAp 2019, TPC Co-Chair of EAI GreeNets 2019, and Workshop Co-Chair of IEEE ICCC/CIC 2019. He was the co-recipient of the ICNC 2018, CSPS 2018, WCSP 2019, and 6GN 2020 Best Paper Awards. He is the current Vice Chair of the Special Interest Group on Green Cellular Networks within the IEEE ComSoc Green Communications and Computing Technical Committee.

Xiu Yin Zhang (Fellow, IEEE) received the B.S. degree in communication engineering from the Chongqing University of Posts and Telecommunications, Chongqing, China, in 2001, the M.S. degree in electronic engineering from the South China University of Technology, Guangzhou, China, in 2006, and the Ph.D. degree in electronic engineering from the City University of Hong Kong, Hong Kong, in 2009.

From 2001 to 2003, he was with ZTE Corporation, Shenzhen, China. He was a Research Assistant from July 2006 to June 2007 and a Research Fellow from September 2009 to February 2010 with the City University of Hong Kong. He is currently a Full Professor and the Vice Dean with the School of Electronic and Information Engineering, South China University of Technology. He is also the Director of the Engineering Research Center for Short-Distance Wireless Communications and Network, Ministry of Education. He has authored or coauthored more than 180 internationally referred journal papers, including more than 100 IEEE Transactions, and 90 conference papers. His research interests include antennas, MMIC, RF components and sub-systems, intelligent wireless communications and sensing.

Dr. Zhang is a Fellow of the Institution of Engineering and Technology (IET). He was the general chair/co-chair/technical program committee (TPC) chair/member and session organizer/chair for a number of conferences. He was the recipient of the National Science Foundation for Distinguished Young Scholars of China. He won the first prize of the 2015 Guangdong Provincial Natural Science Award and 2020 Guangdong Provincial Technological Invention Award. He was the supervisor of several conference best paper award winners. He is an Associate Editor for the IEEE ANTENNAS AND WIRELESS PROPAGATION LETTERS, *IEEE Antennas and Propagation Magazine,* and IEEE OPEN JOURNAL OF ANTENNAS AND PROPAGATION.

Kai-Kit Wong (Fellow, IEEE) received the B.Eng., M.Phil., and Ph.D. degrees in electrical and electronic engineering from the Hong Kong University of Science and Technology, Hong Kong, in 1996, 1998, and 2001, respectively. After graduation, he took up academic and research positions with the University of Hong Kong, Hong Kong, Lucent Technologies, Bell-Labs, Holmdel, NJ, USA, Smart Antennas Research Group, Stanford University, Stanford, CA, USA, and University of Hull, Hull, U.K. He is the Chair of wireless communications with the Department of Electronic and Electrical Engineering, University College London, London, U.K.

His current research focuses on 5G and beyond mobile communications. He was the co-recipient of the 2013 IEEE Signal Processing Letters Best Paper Award and the 2000 IEEE VTS Japan Chapter Award at the IEEE Vehicular Technology Conference in Japan in 2000, and a few other international best paper awards. He is a Fellow of IET and is also on the editorial board of several international journals. Since 2020, he has been the Editor-in-Chief of the IEEE WIRELESS COMMUNICATIONS LETTERS.